Article

Open-Source Data Logger System for Real-Time Monitoring and Fault Detection in Bench Testing

Marcio Luís Munhoz Amorim [1] , Jorge Gomes Lima [2], Norah Nadia Sánchez Torres [3,4] , Jose A. Afonso [5] ,
Sérgio F. Lopes [6] , João P. P. do Carmo [1] , Lucas Vinicius Hartmann [2] , Cicero Rocha Souto [2] , Fabiano Salvadori [2]
and Oswaldo Hideo Ando Junior [2,3,4,]*

[1]   Group of Metamaterials Microwaves and Optics (GMeta), Department of Electrical Engineering (SEL),
    University of São Paulo (USP), Avenida Trabalhador São-Carlense, Nr. 400, Parque Industrial Arnold Schmidt,
    São Carlos 05508-220, SP, Brazil; marciolma@usp.br (M.L.M.A.); jcarmo@sc.usp.br (J.P.P.d.C.)
[2]   Smart Grid Laboratory (LabREI), Center for Alternative and Renewable Research (CEAR), Federal University
    of Paraiba (UFPB), João Pessoa 58051-970, PB, Brazil; jorgeg.lima@cear.ufpb.br (J.G.L.);
    lucas.hartmann@cear.ufpb.br (L.V.H.); cicerosouto@cear.ufpb.br (C.R.S.); salvadori.fabiano@cear.ufpb.br (F.S.)
[3]   Research Group on Energy & Energy Sustainability (GPEnSE), Academic Unit of Cabo de Santo
    Agostinho (UACSA), Federal Rural University of Pernambuco (UFRPE), Cabo de Santo Agostinho 54518-430,
    PE, Brazil; norah.torres@aluno.unila.edu.br
[4]   Interdisciplinary Postgraduate Program in Energy & Sustainability (PPGIES), Federal University of Latin
    American Integration—UNILA, Foz do Iguaçu 85870-650, PR, Brazil
[5]   Center for Microelectromechanical Systems (CMEMS), University of Minho, 4800-058 Guimarães, Portugal;
    jose.afonso@dei.uminho.pt
[6]   Centro Algoritmi (LASI), University of Minho, 4704-553 Guimarães, Portugal; sergio.lopes@dei.uminho.pt
*   Correspondence: oswaldo.ando@ufrpe.br

Abstract: This paper presents the design and development of a proof of concept (PoC) open-source
data logger system for wireless data acquisition via Wi-Fi aimed at bench testing and fault detection
in combustion and electric engines. The system integrates multiple sensors, including accelerometers,
microphones, thermocouples, and gas sensors, to monitor critical parameters, such as vibration,
sound, temperature, and CO_2 levels. These measurements are crucial for detecting anomalies in
engine performance, such as ignition and combustion faults. For combustion engines, temperature
sensors detect operational anomalies, including diesel engines operating beyond the normal range
of 80 °C to 95 °C and gasoline engines between 90 °C and 110 °C. These readings help identify
failures in cooling systems, thermostat valves, or potential coolant leaks. Acoustic sensors identify
abnormal noises indicative of issues such as belt misalignment, valve knocking, timing irregularities,
or loose parts. Vibration sensors detect displacement issues caused by engine mount failures, cracks
in the engine block, or defects in pistons and valves. These sensors can work synergistically with
acoustic sensors to enhance fault detection. Additionally, CO_2 and organic compound sensors
monitor fuel combustion efficiency and detect failures in the exhaust system. For electric motors,
temperature sensors help identify anomalies, such as overloads, bearing problems, or excessive shaft
load. Acoustic sensors diagnose coil issues, phase imbalances, bearing defects, and faults in chain or
belt systems. Vibration sensors detect shaft and bearing problems, inadequate motor mounting, or
overload conditions. The collected data are processed and analyzed to improve engine performance,
contributing to reduced greenhouse gas (GHG) emissions and enhanced energy efficiency. This
PoC system leverages open-source technology to provide a cost-effective and versatile solution for
both research and practical applications. Initial laboratory tests validate its feasibility for real-time
data acquisition and highlight its potential for creating datasets to support advanced diagnostic
algorithms. Future work will focus on enhancing telemetry capabilities, improving Wi-Fi and cloud
integration, and developing machine learning-based diagnostic methodologies for combustion and
electric engines.

1. Introduction

Global greenhouse gas (GHG) emissions have steadily increased, especially in the energy and transportation sectors. Since 1990, global emissions have grown by 41%, with the energy sector responsible for 73% of these emissions. Among them, the transportation sector alone contributes 15% of total emissions, primarily due to fossil fuel consumption in internal combustion engines. In this context, Brazil predominantly relies on a fleet powered by internal combustion engines, underscoring the importance of seeking alternatives and adopting technologies to promote sustainability in the transportation sector. This effort aligns with the Sustainable Development Goals (SDGs) of Agenda 2030 and the commitments of the Paris Agreement for achieving net-zero emissions by 2050. Additionally, Brazil has committed to reducing CO_2 emissions by 37% by 2025, with a target of 43% reduction by 2030 [1–3].

The rapid development of digital technology has brought dramatic changes to many sectors, including the world of internal combustion engines essential for transportation, energy production, and manufacturing. The demand for a greater economy, lower emissions, and higher performance requires the use of advanced engineering, design, and operational management techniques [4,5]. In this sense, developing and implementing advanced techniques using non-invasive sensors are crucial for the widespread adoption of prediction and fault identification systems in internal combustion engines. These technologies aim not only to maximize energy efficiency and reduce operational costs but also play a crucial role in reducing GHG emissions. Effective data management and efficiency improvements enable enhanced operational and maintenance efficiency, prolonging equipment lifespan and mitigating pollutant emissions through optimized real-time operations. This approach not only aligns with global climate mitigation commitments but also drives the transition toward a more sustainable and resilient future [6].

In this context, this paper presents the design and development of a low-cost proof of concept (PoC) to validate its functionality and applicability in recording telemetry data. The collected data are post-processed and analyzed to detect failures in benchtop combustion engines. The proposed PoC is used to validate the efficiency and technical feasibility of the naval telemetry system for coastal shipping, which is part of a broader telemetry platform. This platform consists of an onboard data acquisition system comprising hardware and software, facilitating the telemetry of engines. This solution integrates with a logistics center via the Internet of Things (IoT), providing cloud computing and a real-time control panel. The paper's contributions are summarized as follows:

- Development of an Open-Source Data Logger System: This paper describes the design and implementation of an open-source data logger system for monitoring and fault detection in bench testing of internal combustion engines and electrical engines. This system is equipped to collect and analyze data on vibration, sound, temperature, and CO_2 levels (combustion engines), which are crucial for identifying ignition and combustion faults;
- Proof of Concept (PoC) Validation: The study presents a comprehensive proof of concept (PoC) that validates the functionality and applicability of the data logger system. The PoC demonstrates the system's capability to efficiently acquire data and create datasets for research and development purposes;
- Integration of Non-Invasive Sensors: Implementing non-invasive sensors, such as accelerometers, microphones, thermocouples, and gas sensors, ensures minimal interference with engine operation while providing accurate real-time data for fault detection and monitoring;

- Cost-Effective Solution: By leveraging open-source technology and low-cost components, the developed system offers a cost-effective solution for fault detection and monitoring, making it accessible for a wide range of applications in both research and practical scenarios;
- Future Research Directions: This paper identifies potential future improvements, including the enhancement of Wi-Fi and cloud capabilities for remote telemetry, the creation of comprehensive datasets, and the development of advanced diagnostic methodologies using the collected data. These directions aim to foster innovation and improve the reliability and sustainability of internal combustion engines.

The structure of this article is organized into three main sections, addressing different aspects of telemetry platform development. Section 1 contextualizes the project's objectives, emphasizing the relevance of telemetry in diagnostics fault contexts. Section 2 presents a brief State-of-the-Art discussion of the development of open-source systems and devices using low-cost electronics. Section 3 presents details of the materials and methods used, including the specification and implementation of the PoC, along with preliminary results on the technical feasibility of applying the PoC for fault detection and monitoring of combustion engines in bench testing. Section 4 presents the obtained results and discusses key considerations for future research, exploring potential PoC improvements. Finally, Section 5 presents the conclusions.

Table 1 presents examples of the proposed system's applications. The proposed system also has applications in research laboratories, where it can be used to monitor and analyze electric and combustion engines under controlled conditions. This functionality allows for hypothesis validation and precise data collection, which are essential for developing advanced fault detection algorithms and providing a robust foundation for engineering experiments.

The system shows great potential in the automotive diagnostics sector by identifying engine faults in vehicles using non-invasive sensors. This approach significantly reduces diagnostic time and operational costs while enhancing the effectiveness of predictive maintenance and preventing unexpected failures during vehicle operation.

Education and training: The system can be implemented as a practical tool in engineering courses. Its affordable cost and functional design make it ideal for teaching concepts such as signal analysis and engine diagnostics and fostering innovation and experimentation in academic environments.

Naval and transport sector: In this sector, marine engine telemetry enables remote real-time analysis. This functionality enhances operational efficiency, reduces greenhouse gas emissions, and improves reliability in transport operations, promoting a more sustainable approach.

Industrial platforms: The system can be used for the continuous monitoring of engines, focusing on detecting abnormal vibrations and excessive temperatures. This application is critical for preventing catastrophic failures, extending equipment lifespan, and reducing unplanned operational interruptions.

Renewable energy sector: The system can be applied to diagnose engines in wind turbines or hybrid generation systems. This usage increases energy efficiency, improves integration with IoT systems, and reduces environmental impacts, fostering more sustainable solutions.

Table 2 provides a comprehensive overview of diagnostic techniques used for fault detection in engines, highlighting the sensors employed and the types of faults identified. The methodologies range from discrete transforms, such as Fourier (DFT) and Wavelet (DWT), to advanced machine learning algorithms, like Artificial Neural Networks (MLPs) and Support Vector Machines (SVMs). The sensors used include vibration, acoustic pressure, temperature measurement devices, and portable tools, like smartphone accelerometers, emphasizing the flexibility of these approaches. These techniques enable the identification of critical component failures, such as exhaust valve damage, injector issues, and cylinder head gasket leaks while also addressing mechanical problems, like bearing wear and cylinder leakage. Analyses using methods like Fast Fourier Transform (FFT) and density estimation,

combined with detection algorithms, enhance diagnostic precision, offering non-invasive and scalable solutions for various scenarios, including automotive and marine engines. Integrating sensors and advanced algorithms underscores the potential for optimizing predictive maintenance and preventing catastrophic failures in complex systems.

Table 1. Demonstration and examples of application of the proposed system.
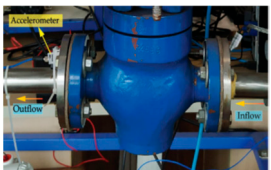
Ref.	Application	Equipment/Sensors	Type of Fault
[7]		CAT G3516B engine—16 cylinders: Tektronix TDS 420 A oscilloscope; magnetic pick-up; Kistler Type 6055BB pressure sensor; and PCB Piezotronics 353B17 accelerometers.	Combustion layer failures, ignition failures, elastic sealing, and mechanical failures.
[8]	Engine from Ford Focus.	IC engine from Ford Focus: chassis dynamometer and Vibration PCB Piezotronics ICP.	Exhaust valve damage, injector damage, and cylinder head gasket damage.
[9]		A four-stroke RUGGERINI RY125 diesel engine; Sulzer 6AL20/24 marine engine; and Woodward PGA-type multi-scope rotational speed controller.	Reliability status.
[10]		ICP 338B34 single-axis piezoelectric accelerometers and a 482A16 PCB® Piezotronics INC amplifier.	IC engine valve clearance diagnosis.
[11]		A single-axis PCB 352C03 ceramic shear ICP accelerometer.	Control valve failure.
[12]	Kubota D905 engine	Kubota D905 3-cylinder engine: Monitran MTN/1100SC constant current accelerometers.	Mechanical failures: big end bearing wear and cylinder leakage.
[13]		Integrated hardware and software platform: Arduino Due and CMA-4544PF-W electret condenser microphone and processing software running on smartphones.	Engine misfires and alternator belt problems.

Table 2. Diagnostic techniques, sensors, and fault types in engine monitoring.

Ref.	Technique	Sensors	Type of Fault
[7]	Discrete Fourier Transform (DFT)	Vibration and acoustic pressure	Combustion layer failures and ignition failures.
[8]	Discrete Wavelet Transform (DWT) and Probabilistic Neural Networks (PNNs)	Vibration and acoustic	Exhaust valve damage, injector damage, and cylinder head gasket damage.
[9]	Support Vector Machine (SVM)	Sensor array	Reliability status.

Table 2. *Cont.*

Ref.	Technique	Sensors	Type of Fault
[10]	Artificial Neural Network Multi-layer Perceptrons (MLPs)	Vibration	Valve clearance classification.
[11]	Fast Fourier Transform (FFT) and Support Vector Machine (SVM)	Vibration	Control valve failures.
[12]	Parzen Windows Density Estimation + One-Class Support Vector Machine (OCSVM)	Vibration and pressure	Mechanical failures: big end bearing wear and cylinder leakage.
[13]	Artificial Neural Network + Discrete Wavelet Transform (DWT) + Fractal Dimension	Vibration and chaos analysis	Engine misfires and alternator belt problems.
[14]	Artificial Neural Network Multi-layer Perceptrons (MLPs) and Probabilistic Neural Networks (PNN)	Vibration and temperature	Combustion and mechanical failures.
[15]	Wavelet Multiresolution Analysis (WMA) and Chaos using maximum density (SAC-DM)	Accelerometer	Misfires.

2. Open-Source Hardware Applications

The development of open-source hardware has revolutionized the approach to creating and utilizing electronic devices, enabling broad access to technology and fostering innovation across various fields. This section presents a brief State-of-the-Art discussion of the development of open-source systems and low-cost electronic devices, highlighting key platforms, their applications, and their impact on research and development.

The Open-Source Hardware Certification Program, or OSHWA (Figure 1a), initiated by Bruce Perens in 1997, marked a significant milestone in the open-source hardware movement [16–18]. This program allowed manufacturers to certify their hardware as open, provided they made the technical documentation available. This initiative aimed to democratize access to hardware by removing barriers such as high costs and licensing fees, making advanced technology accessible to a wider audience, including students, researchers, and hobbyists.
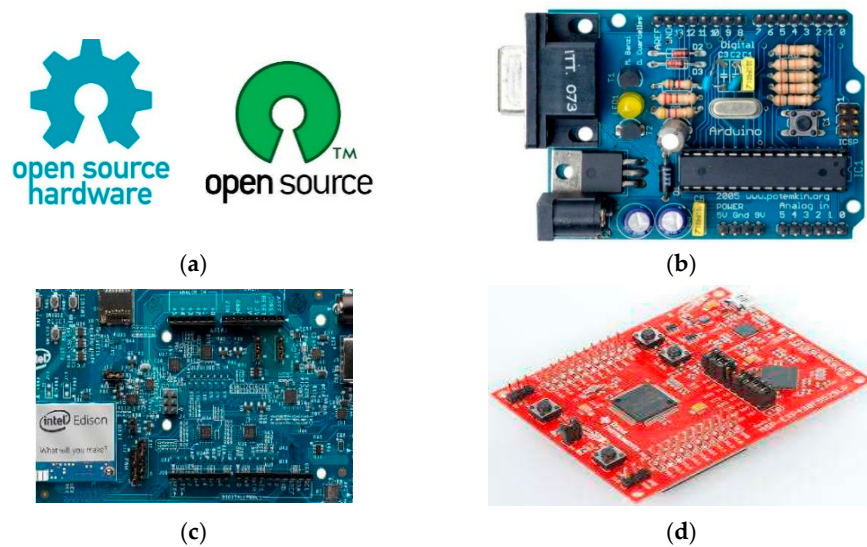
(**a**)

(**b**)
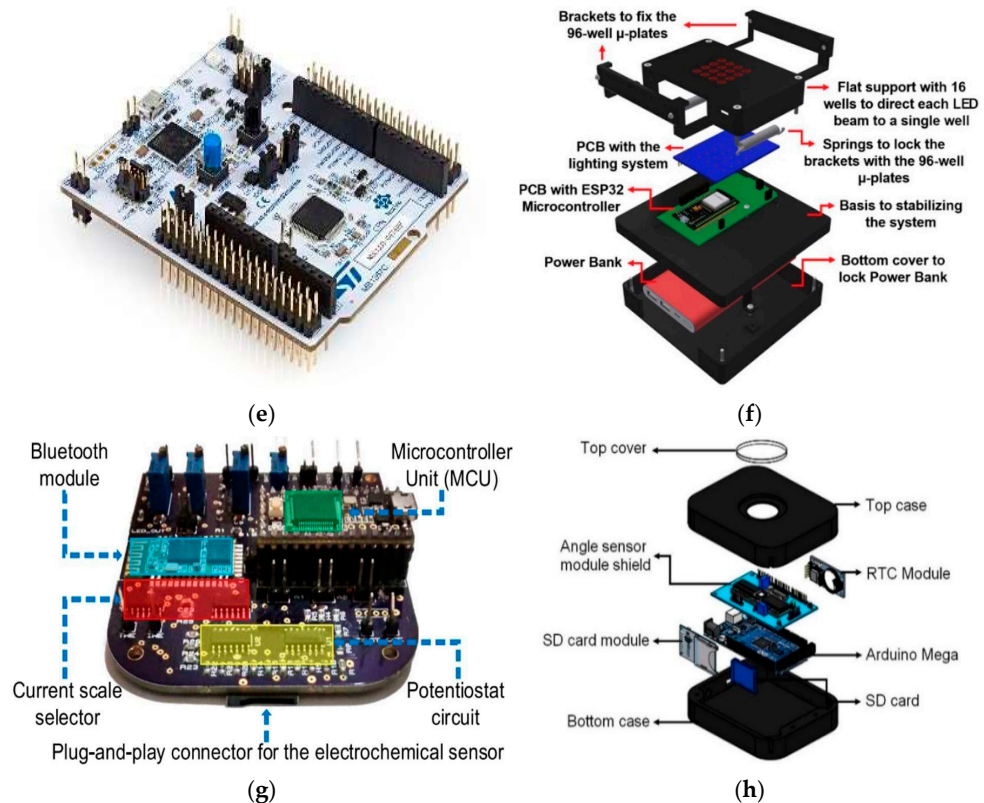
(**c**)

(**d**)

Figure 1. *Cont.*

(**e**)

(**f**)

(**g**)

(**h**)

Figure 1. Examples of development boards and open-source hardware applications: (**a**) Open Source Hardware and Open Source Initiative logos; (**b**) Arduino Uno; (**c**) Intel Edison development board; (**d**) Texas Instruments Launchpad; (**e**) STM32 Nucleon board; (**f**) photodynamic therapy device to detect hepatitis C; (**g**) portable laboratory platform for hepatitis C detection; and (**h**) system for measuring incident light in photovoltaic applications [16–24].

One of the pioneering and most popular projects in the realm of open-source hardware is Arduino (Figure 1b). Launched in 2005, Arduino provides a simple and cost-effective platform for interacting with sensors and actuators, making it ideal for both beginners and professionals. The open-source nature of Arduino has led to a proliferation of projects and applications, ranging from simple educational tools to complex industrial systems [17,18].

The evolution of open-source hardware has seen the development of various platforms, each catering to different needs and applications. Platforms such as Intel Edison Development Board (Figure 1c), Texas Instruments Launchpad MSP430 (Figure 1d), and STM32 Nucleo board [20] with Morph connector for Arduino devices (Figure 1e) have extended the capabilities of open-source hardware, offering powerful development tools and extensive support for various communication protocols and peripherals [16–18].

Figure 1f presents a photodynamic therapy device to detect hepatitis C. This device has 96 wells where blood is deposited, and it uses emitting measures of fluorescent and phosphorescent light to analyze the blood; based on the reflected wavelength light, it is possible to detect the presence of hepatitis C. The picture shows, from the top to the bottom, the wells, the light emitter and sensor PCB, the microcontroller, and the power bank. This open-source hardware has been instrumental in numerous innovative projects, for example, the development of a portable platform for photodynamic therapy that utilizes open-source components, such as the ESP32 microcontroller [21]. This platform enables the selective destruction of cancer cells using light and a photosensitizing drug, showcasing the potential of open-source hardware in medical applications.

Another portable laboratory platform for the detection of Hepatitis C is shown in Figure 1. Instead of having wells to deposit the blood, the device uses a strip similar to those for glucose measurement. A drop of blood is placed in measurement, which is

inserted into the device. The figure shows the Bluetooth module and the current scale selector on the left, the area to insert the strip in the center, and the microcontroller and potentiostat circuits on the right site. This device employs electrochemical biosensors and open-source microcontroller boards to provide rapid and accurate diagnostics. This system demonstrates how open-source hardware can facilitate the development of affordable and accessible healthcare solutions [22,23].

Finally, the system for measuring incident light in photovoltaic applications shown in Figure 1h exemplifies the practical use of open-source hardware in environmental monitoring. This system utilizes an optical sensor to measure the angle and intensity of sunlight, which is crucial for optimizing the positioning and efficiency of solar panels. Incorporating an Arduino Mega for processing, a real-time clock (RTC) for accurate timestamping, and a Secure Digital (SD) card module for data storage, this setup allows for continuous monitoring and precise data logging. Open-source components ensure cost-effectiveness and accessibility, making it a valuable tool for both research and practical applications in renewable energy [24,25].

The use of open-source hardware continues to expand, driven by the maker movement and the increasing availability of low-cost components. Innovations such as the integration of biofuel cells for self-powered sensors and the use of flexible thermoelectric generators highlight the ongoing advancements in this field. These technologies not only enhance the functionality of electronic devices but also promote sustainable and environmentally friendly solutions. The open-source hardware movement has significantly impacted various sectors by providing accessible, cost-effective, and versatile tools for innovation. As technology continues to evolve, the potential for open-source systems and devices to drive further advancements in research, education, and industry remains vast and promising [26,27].

3. Materials and Methods

This section details the procedures used to develop and implement the open-source data logging system for recording data and monitoring faults in bench testing of combustion engines, describing the process of designing and assembling the data acquisition system [28,29].

3.1. PoC Design and Specifications

For the development of this project, considering the use of a low-cost and low computational power approach, and applying non-invasive techniques, there was the possibility of using a low-cost microcontroller. Based on the State of the Art, an ESP32-WROOM32 microcontroller board (Espressif Systems, Shanghai, China) equipped with embedded Wi-Fi was selected that supports a wide range of serial communication protocols, such as I2C and SPI, allowing multiple hardware attachments. Initially, a study was conducted to define the most useful methods for non-invasive measurements, and the methods chosen were as follows: an accelerometer to measure vibration harmonics in the engine; sound to detect valve tapings and loose parts; temperature for coolant problems of excessive loads; CO_2 levels; and organic compounds to detect leaks in exhaustion pipes. A 128×64 pixels OLED (Organic Light-Emitting Diode) display module (Waveshare, Shanghai, China) with an I2C screen and other small components, like switches and buttons, were also included.

Based on a previous study, compatible sensors and modules available in the market providing accurate information were chosen. Figure 2 shows the block diagram of the electronics connections circuit, showing the peripherals and their connection to the ESP32 via I2C (Inter-Integrated Circuit), SPI (Serial Peripheral Interface), GPIO (General Purpose Input/Output), and ADC (Analog-to-Digital Converter), as well as the power supply (with a BMS (battery management system) and two lithium-ion batteries (18650)).
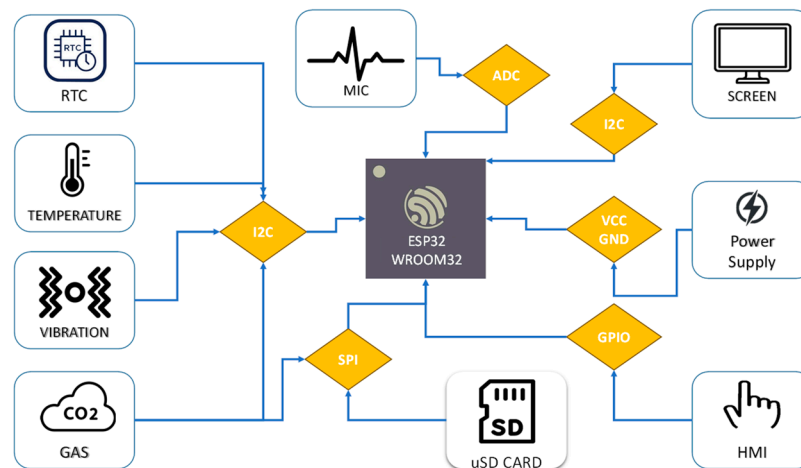
Figure 2. Block diagram of the electronic circuit components and connections.

The ESP32-WROOM32 [30] development board was utilized because of its low cost and intrinsic capabilities. For example, it provides a 12-bit ADC with 18 channels capable of 2-MHz sampling, which allows the PoC to convert the analog signal from the microphone and save it to a Secure Digital (SD) card at a rate of 3.6 M samples per hour in ideal conditions. This allows more efficient detection of small and fast errors. In addition, the ESP32-WROOM32 allows multiple hardware attachments and multiple wireless communication protocols, such as IEEE 802.11/Wi-Fi module (Espressif Systems, Shanghai, China), Bluetooth Low Energy version 5(Espressif Systems, Shanghai, China) , and ESP-NOW (Espressif Systems, Shanghai, China) [31].

Concerning the selected sensors, a microphone module model MAX4466 (Analog Devices, Norwood, MA, USA) [32] was used for acoustic dissipation and mechanical woes that can generate excessive noise from valve taping or loose parts. This microphone has a sound frequency capture range between 20 Hz and 20 kHz and was connected to an amplifier with a 126-dB common-mode rejection ratio (CMMR) and a bandwidth of 200 kHz, which provides the signal to the ADC.

The thermal analysis is based on two temperature sensors. One sensor is external to the engine and uses a MAX6675 (Analog Devices, Norwood, MA, USA) [33] module connected to a type K thermocouple with a measuring range between zero and 1024 °C. The thermocouple can be installed into the motor block or other parts with excessive temperature. It can detect temperature anomalies in the range between 90 °C to 105 °C for gasoline cars and between 88 °C and 99 °C for diesel cars. This sensor communicates through a SPI digital interface using three wires.

The other temperature sensor is based on the ENS160 (ScioSense, Eindhoven, Netherlands) [34] module and communicates with the ESP32 using an I2C digital interface. It is capable of measuring temperatures between -40 °C and 85 °C, as well as relative humidity. This temperature sensor was added to protect the PoC from excessive heat, allowing it to trigger an alarm in the case of the unit being exposed to excessive heat or moisture.

The equivalent CO_2 (eCO_2) and total volatile organic compound (TVOC) measurements were also acquired using an ENS160 module. They allow the PoC to detect containment failures and inefficient fuel combustion. This module is placed in the PoC and detects gases outside the motor.

To detect vibrations outside the harmonical vibration of the motor operation mode, a digital accelerometer was added. The used device, model ADXL345 (Analog Devices, Norwood, MA, USA), has 3 axes, a measurement range of ±2 g, a resolution of 13 bits, and a sampling rate of 3200 Hz.

To ensure the precise timing of each event, the DS3231 (Maxim Integrated, Norwood, MA, USA) [35], an RTC with I2C interface, was chosen. It allows each sample to be correctly marked with the date and time.

The integration of sensors tailored to specific engine types allows for comprehensive monitoring and fault detection. For combustion engines, the focus lies on identifying inefficiencies in mechanical and combustion processes, while for electric motors, the emphasis is on diagnosing electrical and mechanical anomalies. Below are the detailed applications for each engine type.

Combustion engines require a diverse set of sensors to monitor critical operational parameters, ensuring efficient performance and timely detection of faults. The sensors are designed to identify issues related to thermal regulation, structural integrity, and exhaust efficiency [36,37].

Temperature Sensor: Detects operational anomalies in diesel engines operating beyond the normal range of 80 °C to 95 °C and gasoline engines between 90 °C and 110 °C. These measurements are critical for identifying failures in the cooling system, thermostat valves, or potential coolant leaks.

Acoustic Sensor: Identifies abnormal noises that may indicate issues, such as misaligned belts, valve knocking, timing irregularities, or loose components. This sensor helps diagnose mechanical inconsistencies that can compromise engine performance.

Vibration Sensor: Detects displacement-related issues, such as failures in engine mounts, cracks in the engine block, or defects in pistons and valves. When combined with acoustic sensors, it provides a more comprehensive fault detection mechanism.

Organic Compound and CO_2 Sensors: Monitor fuel combustion efficiency and detect failures in the exhaust system, ensuring proper burning performance and reducing emissions.

Electric motors operate differently from combustion engines, relying heavily on electrical components and mechanical integrity. The sensor system focuses on identifying electrical irregularities and mechanical wear to optimize performance and prevent damage.

Temperature Sensor: Monitors operational anomalies, including overload conditions, bearing problems, or excessive shaft loads that can lead to mechanical failure.

Acoustic Sensor: Diagnoses coil irregularities, phase imbalances, bearing defects, or faults in chain and belt systems, ensuring smooth motor operation.

Vibration Sensor: Detects issues such as shaft misalignments, bearing wear, insufficient motor mounting, or overload conditions, helping to prevent motor inefficiencies and failures.

Memory for the PoC is provided using a Class10 (UHS-I) MicroSD (generic, Shanghai, China) card with 16 gigabytes inserted into an SD card reader/writer. This module uses SPI and can record data with speeds up to 40 MHz

The power supply is provided by a BMS (battery management system) (generic, Shanghai, China) [38] connected to two 18650 lithium-ion batteries with a total of 2500 mAh, allowing the PoC to operate between 8 and 12 h. The average power usage of the PoC is between 180 mAh and 240 mAh, averaging at 200 mAh.

$$Time = \frac{Total\ Current}{PoC\ Current} = \frac{2500\,\text{mAh}}{200\,\text{mAh}} = 12.5\,\text{h} \tag{1}$$

The power supply performance may vary depending on factors such as battery lifespan, specific code compilations, and operational conditions. The average power consumption of 200 mAh is an extrapolation based on ideal conditions. Additionally, the internal temperature sensor plays a critical role in ensuring device safety by monitoring thermal conditions. If the system detects that the PoC is operating outside optimal temperature ranges, it triggers an alert to prevent overheating. This mechanism helps maintain the device's functionality and extends the battery's operational lifespan.

The human–machine interface (HMI) combines the OLED screen, which can display all relevant information, with a 5-position joystick and a button, both connected to the ESP32 via GPIO pins. The joystick and the button can be customized in the code to perform any required interaction.

To demonstrate that the proposed device is a low-cost product, Table 3 shows the costs per part in dollars and the total price. The prices are based on common marketplaces and websites that provide worldwide shipping and cost-effective prices.

Table 3. Cost of the device's parts and components.

PART	MODEL	PRICE
ESP32	ESP32-WROOM-32S (Espressif Systems, Shanghai, China)	USD 2.37
Microphone	MAX4466 (Analog Devices, Norwood, MA, USA)	USD 1.26
Temperature sensor	MAX6675 (Analog Devices, Norwood, MA, USA)	USD 1.45
Gas sensor	ENS160 (ScioSense, Eindhoven, The Netherlands)	USD 3.61
Accelerometer	ADXL345 (Analog Devices, Norwood, MA, USA)	USD 0.94
RTC	DS3231 (Maxim Integrated, Norwood, MA, USA)	USD 0.81
MicroSD	OEM (generic, Shanghai, China)	USD 2.01
BMS	15W UPS module (generic, Shanghai, China)	USD 3.12
OLED	128 × 64 OEM	USD 2.11
Batteries (x2)	18650 OEM (generic, Shanghai, China)	USD 2.70
Joystick	OEM (generic, Shanghai, China)	USD 1.24
Switch	OEM (generic, Shanghai, China)	USD 0.25
Case	Aluminum (generic, Shanghai, China)	USD 1.80
Wires	OEM (generic, Shanghai, China)	USD 0.50
Filament	PLA (Polylactic Acid) (generic, Shanghai, China)	USD 1.00
Screws	M3 (generic, Shanghai, China)	USD 0.60
Total		USD 28.47

3.2. PoC Hardware and Assembly

This section presents the prototyping of the proof of concept (PoC) for the data acquisition system focused on the monitoring and fault detection of engines. Structurally, the PoC includes a perforated PCB (perfboard) for component accommodation, AMG20 wires, a battery charging module, an ON/OFF switch, a PLA filament for 3D printing of the part that houses the PCB and modules, and an aluminum profile to assemble all components into a single device.

The PoC components were soldered onto a perfboard. Figure 3 shows the perfboard with its daughter boards: (a) an ESP32 with the USB interface facing out; (b) a MicroSD card reader/writer, also facing out in the same direction; (c) an RTC module with a coin cell to keep time even without the power supply; (d) an accelerometer, placed into the exact center of the device, to obtain proper measurements when the board is placed on top of a motor; (e) a thermocouple sensor controller; (f) a header connector for the external microphone (analog) and an external I2C for the ENS160; (g) a header for the external HMI OLED screen and the gas sensor both with I2Cs and for the Joystick with 6 digital signals; and (h) a power supply rated to 5 V and GND.

The HMI components were soldered under the board with wires and solder traces. Figure 4 shows all the components attached without the external enclosure: (a) the main PCB; (b) the microphone and the temperature sensor connected to a side part; (c) the cable for connection to external sensors and the HMI; (d) the frontal part of the HMI, showing the OLED screen, gas sensor, and Joystick buttons; (e) the battery module; (f) the external thermocouple; and (g) the connection cables for the thermocouple and the batteries.
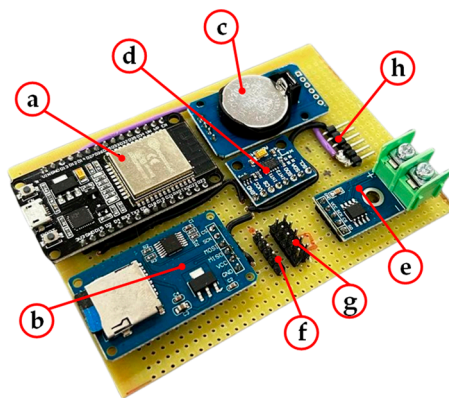
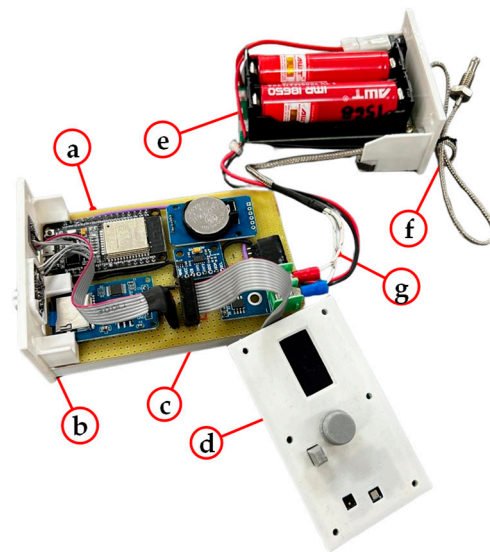**Figure 3.** Perfboard with the daughter boards attached.

Figure 4. Mainboard and peripheral boards.

The design used PLA filaments and 3D printing to produce custom design fittings for accommodating the PCB, the battery, and the other components. These fittings and supports were also designed to connect to an enclosure with a rectangular aluminum profile to maintain structure stability in the application environment. Figure 5 shows (a) the enclosure made of an aluminum profile; (b) the cut area for the HMI components; and (c) the internal structure of the PoC.
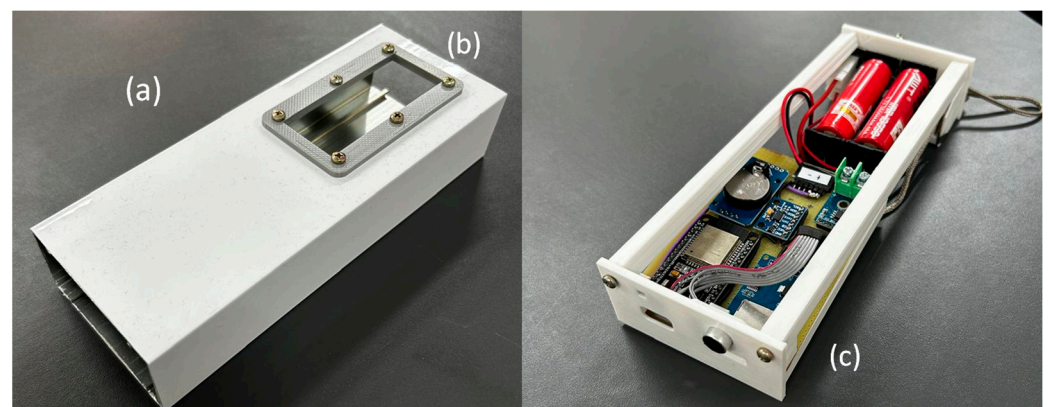

Figure 5. External and internal structures of the PoC device.

Figure 6 showcases the fully developed prototype hardware. Figure 6a shows the left side of the PoC with the mainboard and the left side sensors (mic and temp), and Figure 6b shows the final assembled PoC. Figure 6c shows the left side, with the Mic and temperature sensor. Figure 6d shows the right side, with the power switch, the thermocouple cable, and the USB-C connection to charge the battery cells.
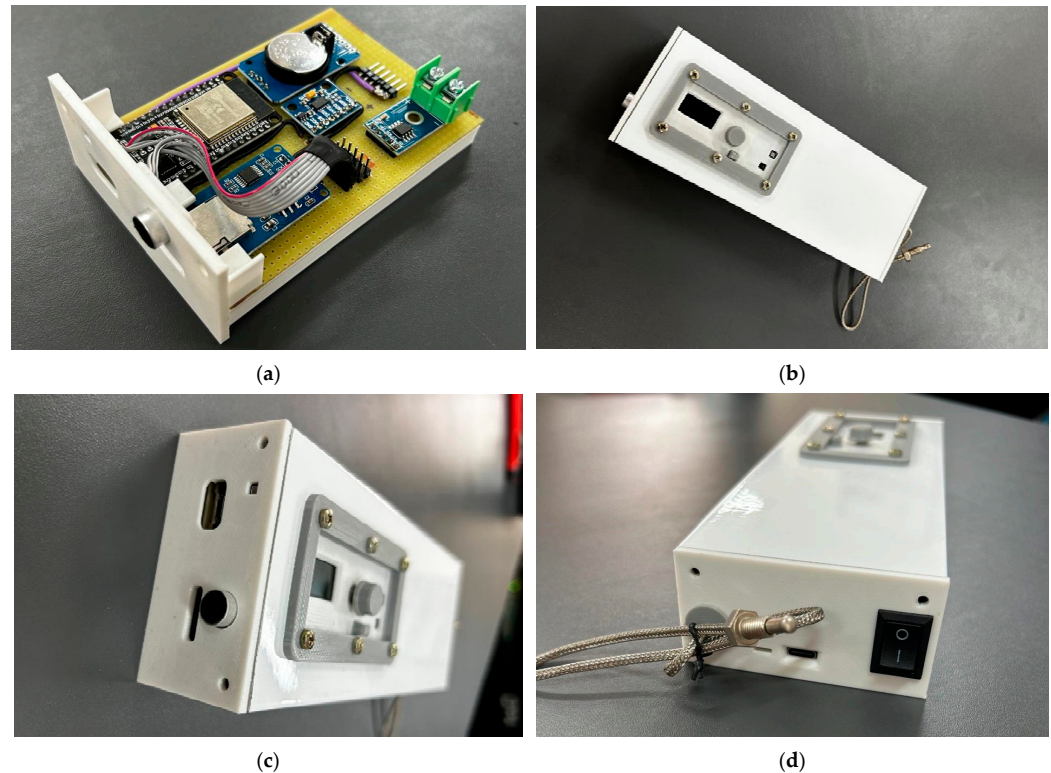

(a)

(b)

(c)

(d)

Figure 6. Overview of the structural components and parts of the PoC.

3.3. PoC Programming Code

The software was developed using Arduino IDE. The objective of this first interaction was to integrate the code of each sensor and module, enabling the prototype to capture information from all sensors simultaneously during testing. Before conducting comprehensive prototype tests with all sensors, it is essential to evaluate the functionality of each sensor individually. This ensures that the code can properly communicate with the hardware. Initial tests showed the firmware working correctly without losing data, crashing, or not recording data. A new version of the code will be implemented in the future to utilize all the hardware capabilities. The code developed and implemented in the data acquisition system is available in Open-Source Code: Data Logger System for Monitoring and Fault Detection in Bench Testing (V.1). Zenodo [39].

Figure 7 shows the block diagram of the code. When the POWER ON switch is pressed, the ESP32 starts the boot, initializes the external hardware, I2C, and SPI, and checks the RTC. If one of these steps fails, the code displays an error message and stops; otherwise, it continues, displaying the sensor values on the screen and waiting for user interaction. If the user presses the button, the code starts to save data on the SD card; if the button is pressed again, the code ends the recording and waits for user action. The screen also displays a progressive timer between presses so the user knows how long the code has been running.

The IoT wireless connection can use the ESP-NOW protocol, and it was also tested to evaluate the distance range. In this setup, the PoC device sends random data to another ESP32 via ESP-NOW, and this ESP32 is connected to a computer via a serial port. The tests showed that the ESP32 running ESP-NOW was able to send data uninterruptedly for a

distance of 15 m. The computer may act as an IoT server, allowing the collected data to be accessed remotely through the Internet.
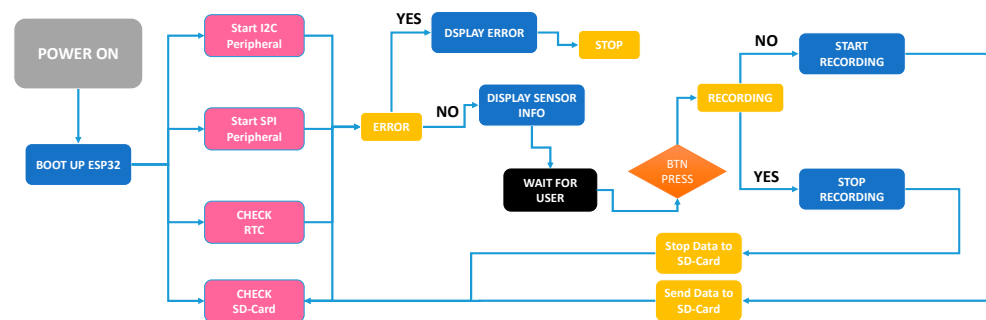

Figure 7. Block diagram of the code behavior.

4. Results and Discussion

This section presents the experimental tests performed to evaluate the performance and validate the proof of concept (PoC) implementation of the proposed data acquisition system. These experiments utilized an ESP32 microcontroller along with various non-invasive sensors in a controlled laboratory environment. The results demonstrate the successful capture of critical parameters, such as vibration, sound, and temperature levels, which are essential for identifying operational anomalies. Integration of the ESP32 facilitates continuous real-time data acquisition, enhancing the system's analytical capabilities.

The system's compact size, battery operation, and wireless connectivity allow it to be used in various environments. It can be secured using clips, nylon straps, magnets, or other methods. For combustion engines, it can be installed under car hoods, within the engine rooms of vessels, or inside truck cabs. Telemetry data can be monitored on a computer via Bluetooth or Wi-Fi. Additionally, due to its built-in thermal sensor, the operator can halt testing in case of overheating to protect the PoC.

The experiment was set up to collect the initial data points of the PoC on an electrical motor in a high-power laboratory. Figure 8 shows the test setup, comprising a three-phase electrical motor attached to a load, with the PoC fastened at the top. Not visible in the picture is the temperature probe connected to the motor's external case.
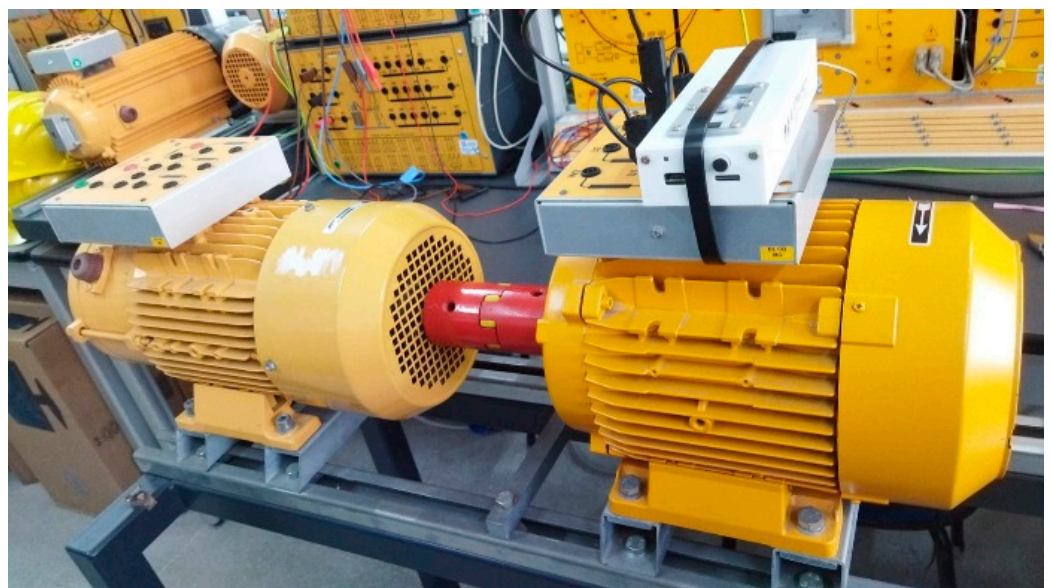

Figure 8. Overview of the structural test setup.

The experiment aims to check the capability of the PoC in recording data in a controlled environment. The developed dataset was divided into three operational modes for data collection using the telemetry device. The setup consists of a DL2050 bench induction motor, a DL2066A bench generator, a DL1017R resistive load, and other necessary instruments for measuring voltage, current, and power, all produced by Delorenzo.

The telemetry device was mounted and fastened on the top of the bench motor, and the collected data included sound and vibration. A MAX4466 microphone module was used for sound acquisition, while a three-axis ADXL345 accelerometer module was used for vibration measurement, and for temperature, the MAX6675 was used.

Partial results can be seen in the charts below, where 1000 samples of noise coming from the engine were collected. Figure 9 shows the RAW signal representing different sound levels of the testing modes. The signal floats at the value around 1700, allowing the positive and negative audio components to be recorded. The baseline, corresponding to the engine without any load, shown in blue, shows a minimum variation during the capture. The second is the engine with the generator, in red, causing more noise to the system, with a large dispersion but not too massive. The last is the engine with load, in yellow, which causes a very high noise, as noticed throughout the entire capture.
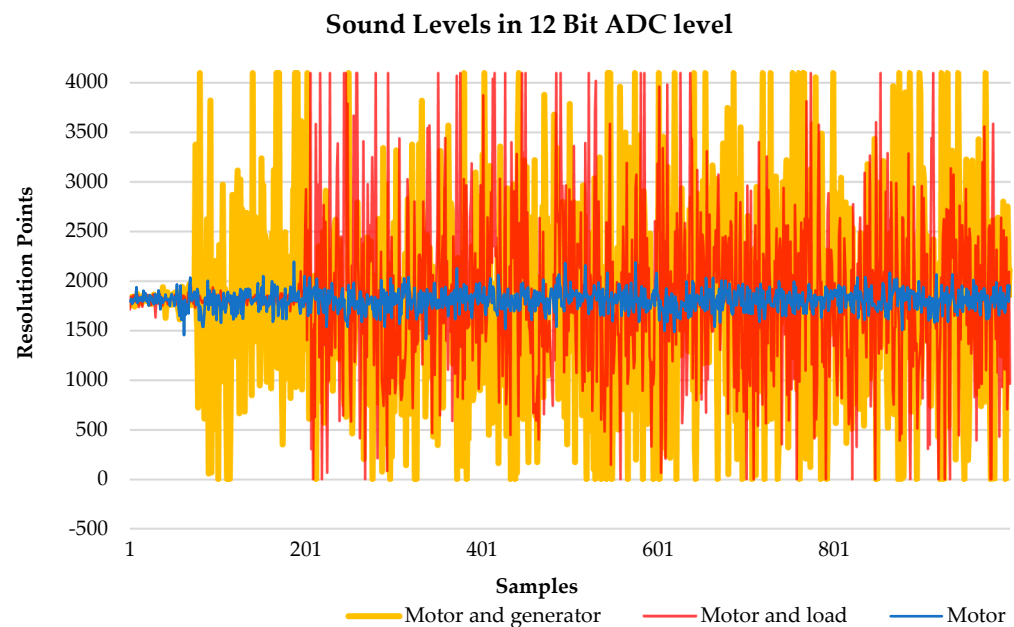

Figure 9. Sound levels of the motor (blue), motor and load (red), and motor and generator (yellow).

It was also observed during these tests that the noise coming from the motor reached the peak range of the microphone, which means that the gain must be lowered in order to properly record all levels. This record was also made in binary values from the ADC. The goal of this test was to gather RAW signals to validate the system, after which post-processing can be performed. The RAW signal represents the microphone noise capture. The goal is not to obtain values in decibels but to map and create a systematic comparison with absolute values of different levels of noise and, as a final analysis, obtain, as a comparison, the values in decibels. As an example, the decibel value can be calculated using the process below, starting with the conversion of the ADC reading to the corresponding voltage through Equation (2):

$$V_{out} = \frac{ADC_{value}}{4095} \times Vref \tag{2}$$

where ADC_{value} is the ADC reading from the microphone, and *Vref* is the reference voltage from the ADC microcontroller, in this case, 3.3 V, and 4095 is the 12 bit full-scale ADC value. As an. For example, the peaks were 3860, but the signals floated at 1700.

$$V_{out} = \frac{3860 - 1700}{4095} \times 3.3v = 1.75v \tag{3}$$

Converting it into decibel levels uses a logarithmic scale to a power level; we can approximate it using Equation (4):

$$dB = 20 \times log_{10}\left(\frac{Vout}{Vref}\right) dB = 20 \times log_{10}\left(\frac{1.75v}{3.3v}\right) = 10.60db \tag{4}$$

Figure 10 shows the vibration of the motor related to the axes X (Figure 10a) and Y (Figure 10b) over time. This test also collected 1000 samples from each method correlating the same axes. The values are in meters per second square acceleration or m/s^2, which means the force that the accelerometer traveled in each direction and not the distance. The first chart makes it possible to show the acceleration of the X-axis. As a baseline, the motor in blue without load has no significant movement, and the motor with load has a wide dispersion of force reaching some peaks of ± 8 m/s^2 for each direction. The motor with a generator had even move acceleration, reaching peaks of ± 11 m/s^2. The second chart is very similar and shows the Y-axis also with the same configuration. As a baseline, the motor in blue without load shows no significant movement, and the motor with load and the motor with the generator are very similar in this chart, both reaching an acceleration of ± 12 m/s^2, which is not very different from the X-axis.

Initial laboratory tests validated the prototype's functionality, affirming its efficacy. The utilization of open-source technology and non-invasive sensors not only proved efficient but also cost-effective, which is crucial for broad application across different contexts.

The PoC was successfully confirmed as a working and functional device. It was assembled and programmed according to the chronogram. The size of the PoC allows it to be easily mounted on a motor. The code made the user interface easy to operate, and the initial results prove that the PoC can be used as a non-invasive device for future tests.

The development and application of this PoC for benchtop data acquisition presents a promising strategy for fault detection and operational monitoring of engines in the field. Based on these initial findings, ongoing adjustments and enhancements are planned to meet research requirements and improve system performance.

Future research may build upon this approach by conducting tests under real-world operational conditions for combustion engines. Establishing a comprehensive dataset from the collected telemetry data will be crucial for advancing non-invasive diagnostic methodologies and developing robust fault detection algorithms. This dataset will foster technological innovation by providing the foundation for more accurate and predictive diagnostics. Additionally, the next phase of development will focus on implementing full Wi-Fi and cloud capabilities to enhance remote telemetry and data accessibility.

Fault tolerance in the system will be achieved through the integration of a robust dataset and machine learning models. Once the dataset is created and the machine learning algorithm is trained, the system will be capable of detecting patterns and subtle, imperceptible faults that may otherwise go unnoticed but could escalate into significant issues over time. The system currently includes internal storage via an SD card, enabling reliable data retention. Future enhancements will provide remote data access through network connections or a cloud-based system, which is yet to be implemented.
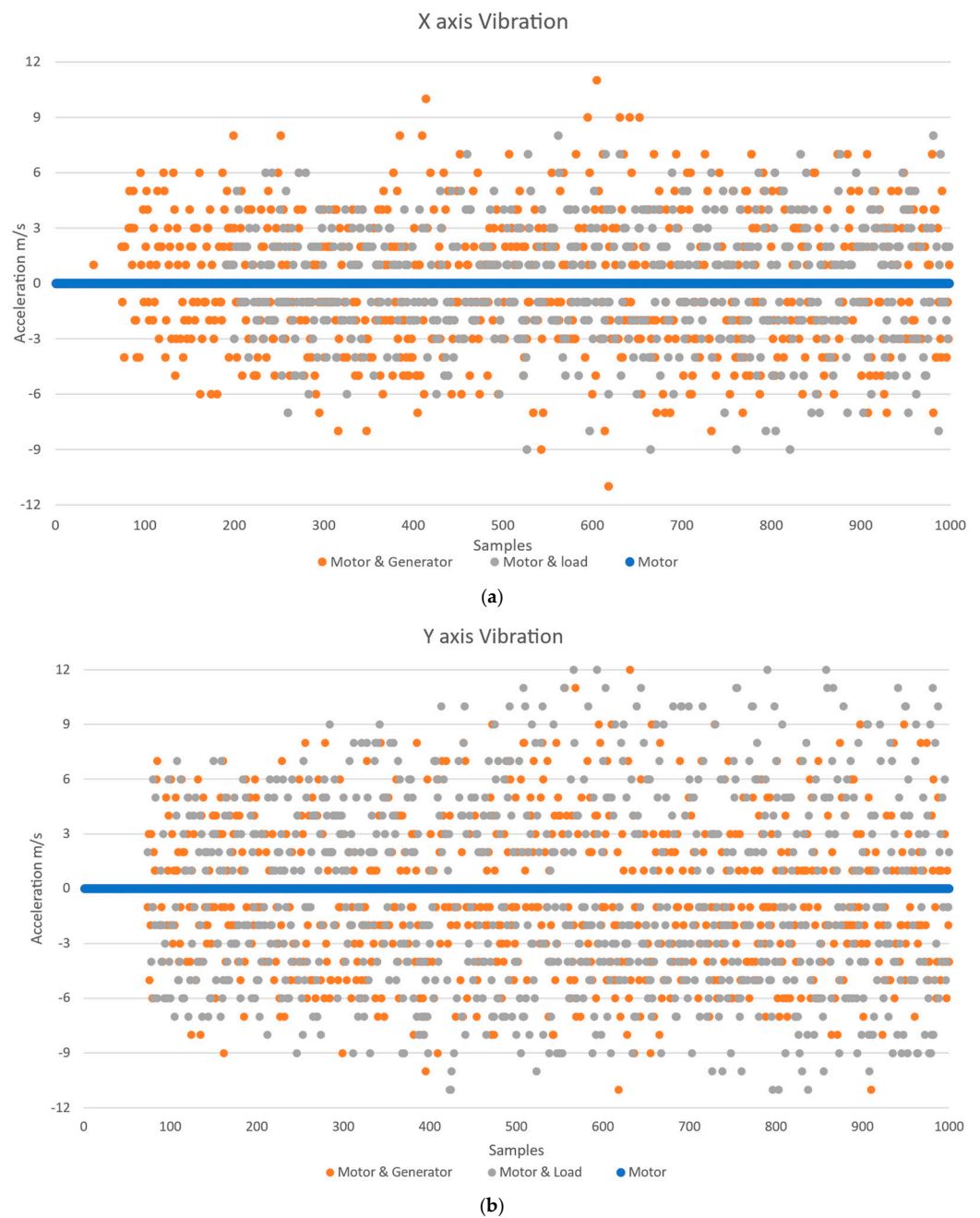
(**a**)

(**b**)

Figure 10. Overview of the vibration dispersion over time between motor, load, and generator in (**a**) x-axis and (**b**) y-axis.

Figure 11 shows the temperature dispersion of the PoC. This test was performed with the external probe installed in the motor case. It tested the motor, the motor with the generator, and the motor with the generator and load. The test was performed in a nonstop method, and it took 15 min, in increments of 5 and 5 min, with 5 min with the motor only, 5 min with the motor and generator, and 5 min with the motor, generator, and load. The figure shows the motor only average of 26.2 °C with SD ± 0.5 °C; the motor and generator average of 26.7 °C, with SD ± 1.0 °C s; and the motor, generator, and load average of 27.8 °C, with SD ± 2.2 °C. This test proves that the PoC can monitor temperature at different stages and is capable of measuring temperatures. The probe can go up to 1024 Celsius, much higher than the melting point of any electrical or combustion motor.
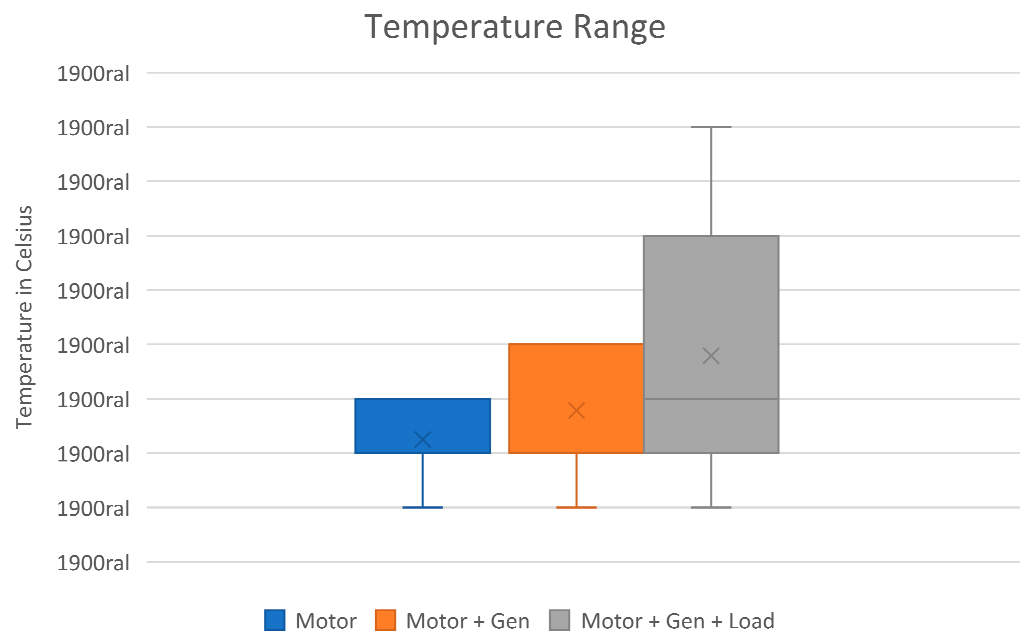
Temperature Range

Figure 11. Overview of the temperature difference between motor, generator, and load.

5. Measurements and Analysis

The system's data analyses were performed remotely, with Fast Fourier Transform (FFT) processing, and graph generation was managed by external models. Data collected from the PoC were extracted and processed externally to provide actionable insights. An internal model, which is yet to be implemented, will deploy TensorFlow Lite Micro on the ESP32 microcontroller. This approach requires a larger sample dataset to train the machine learning model effectively. Once the dataset is created, it will be fed into TensorFlow [23] to optimize data processing, reducing the volume of output data while enabling more precise and efficient decision-making.

To prevent data loss, the system employs an SD card for secure data storage. The ESP32 microcontroller accesses the SD card to open, write, and close files during data recording. This process ensures that previously saved data remains intact, even during the writing phase.

The data collected by the hardware offer a deeper understanding of motor behavior. Initial analysis indicates that the motor was operating under normal conditions during the tests. Advanced analytical tools, such as FFT, were utilized to provide additional insights into engine performance. Future developments aim to incorporate more sophisticated analytical techniques, including real-time machine learning algorithms implemented via TensorFlow [23]. This advancement will enhance fault detection accuracy, allowing the system to identify subtle anomalies, such as excessive friction, loose components, or abnormal temperatures, at early stages. Early detection of such issues has the potential to prevent critical failures and extend engine lifespan.

Figure 12 displays the FFT response from the accelerometer, represented as a spectrogram that shows variations in frequency intensity across multiple periods. In this visualization, warmer colors indicate higher frequency intensities, while cooler colors represent lower intensities. This analysis is useful for identifying periodic patterns and dominant frequencies in low-frequency signals over time, offering valuable insights into the motor's operational characteristics.

Figure 13 displays the FFT analysis of microphone data from the motor. The graph indicates a low-frequency signal with a uniform intensity distribution over time, showing little to no abnormal peaks or noticeable noise. This consistent pattern suggests stable motor operation, with no significant anomalies in sound intensity that might indicate mechanical issues or irregularities.
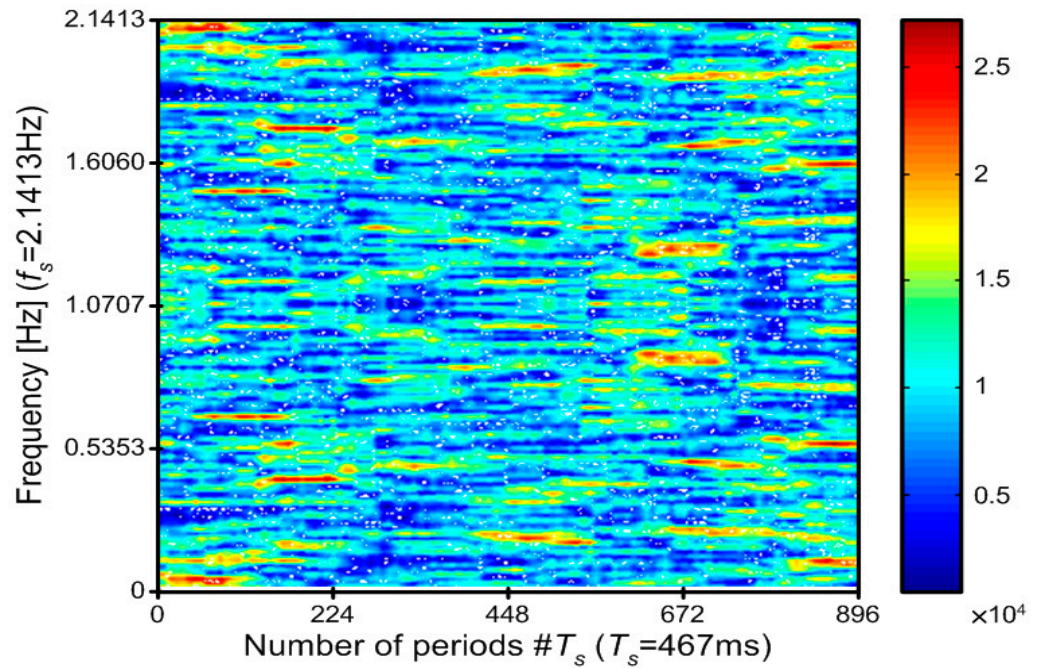
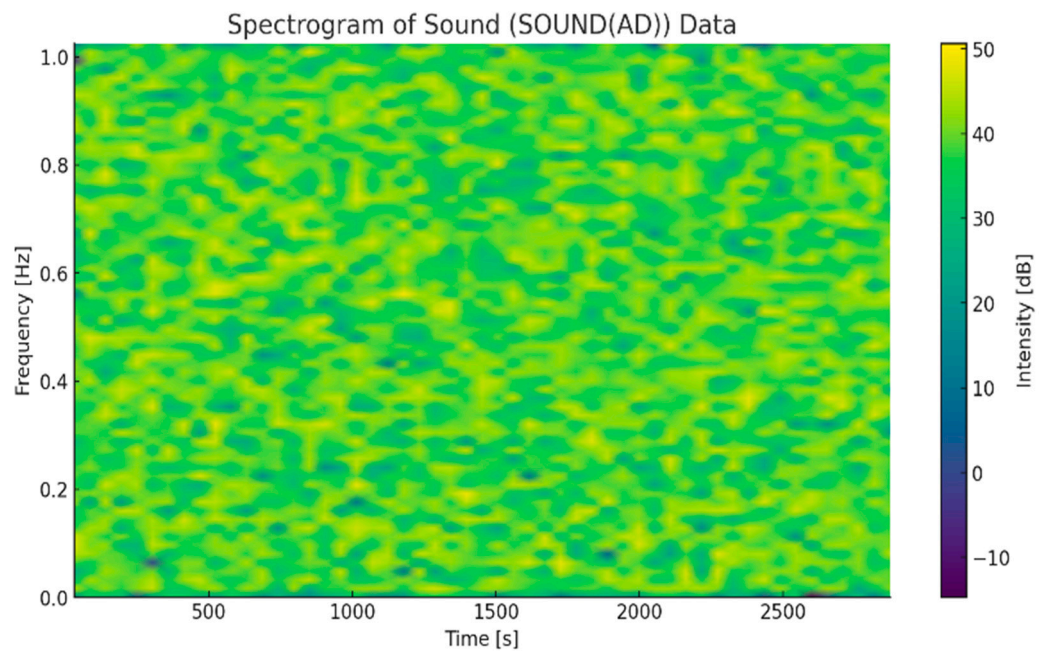**Figure 12.** The FFT response from the accelerometer.

Figure 13. The FFT response from the microphone.

6. Conclusions and Future Perspectives

This paper describes the design and development of a proof of concept (PoC) data logger system for bench testing aimed at detecting faults in combustion and electric engines. The initial validation results confirm that the PoC is a functional and reliable device assembled and programmed within the planned timeline. Its compact size allows easy installation in a wide range of engines, and its intuitive user interface enhances usability. The adoption of open-source technology and non-invasive sensors demonstrates efficiency and cost-effectiveness, positioning the system as a versatile tool for research and industrial applications.

The initial laboratory tests validate the system's ability to measure critical parameters, such as noise, temperature, and vibration, highlighting its potential as a non-invasive diagnostic tool for deployment in diverse operational settings. The PoC's application for benchtop data acquisition represents a promising approach for real-time fault detection and operational monitoring in engines. However, further refinements are needed to address evolving research needs and maximize system performance.

This proof of concept (PoC) has shown success in controlled environments. It remains in the development phase, with significant improvements planned. The next phase focuses on generating a robust dataset from multiple motor models with diverse telemetry profiles. While this process presents logistical challenges and resource constraints, creating a comprehensive dataset is vital for advancing non-invasive diagnostic methods and developing fault detection algorithms.

To enhance the system's capabilities and expand its applicability, several advancements are planned as follows:

Dataset Creation: A critical step involves collecting telemetry data from various combustion and electric engines, potentially introducing intentional faults to create a dedicated fault dataset. This approach aims to enable more precise diagnostics and predictive fault identification.

TensorFlow Lite Micro Implementation: TensorFlow Lite Micro will be deployed on the ESP32 microcontroller, enabling machine learning models to detect subtle anomalies that might go unnoticed by humans. Once trained, these AI models will refine fault detection accuracy.

TensorFlow Lite Micro Implementation: Periodic cloud backups will be established to ensure secure data storage. This enhancement will enable remote data access and add an extra layer of fault tolerance.

Raspberry Pi Piggyback: A supplementary server module will be developed using Raspberry Pi 5. The PoC will transmit data via Wi-Fi to this module, which will manage storage, perform cloud backups, and execute advanced AI models using the full version of TensorFlow.

Cloud Backup Implementation: Periodic cloud backups will be established, allowing data to be sent to an online server as a secure storage solution.

Human–Machine Interface (HMI): The current interface will be enhanced with a mobile application and an HTTP-based interface, allowing users to monitor the system's performance and progress through cloud services.

These planned advancements will significantly enhance the system's versatility and robustness, making it more suitable for practical applications. By combining machine learning, cloud integration, and advanced telemetry, this PoC has the potential to revolutionize engine diagnostics and monitoring. These developments will not only improve fault detection accuracy but also promote the adoption of open-source, cost-effective technologies across industrial and academic sectors.

Pernambuco (UFRPE). N.N.T.S was funded by the Federal University of Latin American Integration (UNILA).

Data Availability Statement: Data are contained within the article.

Conflicts of Interest: The authors declare no conflicts of interest.

References

1. IEA; IRENA; UNSD; World Bank; WHO. *Tracking SDG 7: The Energy Progress Report*; Policy Commons: Washington, DC, USA, 2024.
2. Sachs, J.; Kroll, C.; Lafortune, G.; Fuller, G.; Woelm, F. *Sustainable Development Report 2022*, 1st ed.; Cambridge University Press: Cambridge, UK, 2022. [CrossRef]
3. CODS. *Índice ODS 2022 para América Latina y el Caribe*; Centro de los Objetivos de Desenvolvimento Sustentável para América Latina e o Caribe: Bogotá, Colombia, 2023; p. 10.
4. Lim, K.Y.H.; Zheng, P.; Chen, C.-H. A state-of-the-art survey of Digital Twin: Techniques, engineering product lifecycle management and business innovation perspectives. *J. Intell. Manuf.* **2020**, *31*, 1313–1337. [CrossRef]
5. Stoumpos, S.; Theotokatos, G.; Mavrelos, C.; Boulougouris, E. Towards Marine Dual Fuel Engines Digital Twins—Integrated Modelling of Thermodynamic Processes and Control System Functions. *JMSE* **2020**, *8*, 200. [CrossRef]
6. Tran, V.D.; Sharma, P.; Nguyen, L.H. Digital twins for internal combustion engines: A brief review. *J. Emerg. Sci. Eng.* **2023**, *1*, 29–35. [CrossRef]
7. Barelli, L.; Bidini, G.; Buratti, C.; Mariani, R. Diagnosis of internal combustion engine through vibration and acoustic pressure non-intrusive measurements. *Appl. Therm. Eng.* **2009**, *29*, 1707–1713. [CrossRef]
8. Czech, P.; Wojnar, G.; Burdzik, R.; Konieczny, Ł.; Warczek, J. Application of the discrete wavelet transform and probabilistic neural networks in IC engine fault diagnostics. *J. Vibroengineering* **2014**, *16*, 1619–1639.
9. Pająk, M.; Kluczyk, M.; Muślewski, Ł.; Lisjak, D.; Kolar, D. Ship Diesel Engine Fault Diagnosis Using Data Science and Machine Learning. *Electronics* **2023**, *12*, 3860. [CrossRef]
10. Jedliński, Ł.; Caban, J.; Krzywonos, L.; Wierzbicki, S.; Brumerčík, F. Application of vibration signal in the diagnosis of IC engine valve clearance. *J. Vibroengineering* **2015**, *17*, 175–187.
11. Venkata, S.K.; Rao, S. Fault Detection of a Flow Control Valve Using Vibration Analysis and Support Vector Machine. *Electronics* **2019**, *8*, 1062. [CrossRef]
12. Smart, E.; Grice, N.; Ma, H.; Garrity, D.; Brown, D. One Class Classification Based Anomaly Detection for Marine Engines. In *Intelligent Systems: Theory, Research and Innovation in Applications*; Studies in Computational Intelligence; Jardim-Goncalves, R., Sgurev, V., Jotsov, V., Kacprzyk, J., Eds.; Springer International Publishing: Cham, Switzerland, 2020; Volume 864, pp. 223–245. [CrossRef]
13. Lima, T.L.d.V.; Filho, A.C.L.; Belo, F.A.; Souto, F.V.; Silva, T.C.B.; Mishina, K.V.; Rodrigues, M.C. Noninvasive Methods for Fault Detection and Isolation in Internal Combustion Engines Based on Chaos Analysis. *Sensors* **2021**, *21*, 6925. [CrossRef]
14. Chen, J.; Randall, R.B.; Feng, N.; Peeters, B.; Van der Auweraer, H. Automated diagnostics of internal combustion engine using vibration simulation. In Proceedings of the ICSV20, Bangkok, Thailand, 7–11 July 2013.
15. Rodrigues, N.F.; Brito, A.V.; Ramos, J.G.G.S.; Mishina, K.D.V.; Belo, F.A.; Filho, A.C.L. Misfire Detection in Automotive Engines Using a Smartphone through Wavelet and Chaos Analysis. *Sensors* **2022**, *22*, 5077. [CrossRef]
16. Debian.org. Announcing: The Open Hardware Certification Program. 2024. Available online: https://lists.debian.org/debian-announce/1997/msg00026.html (accessed on 28 November 2024).
17. Opensource.com. What is Open Hardware. 2013. Available online: https://opensource.com/resources/what-open-hardware (accessed on 21 October 2024).
18. OSHWA.org. Brief History of Open Source Hardware Organizations and Definitions. 2022. Available online: https://www.oshwa.org/research/brief-history-of-open-source-hardware-organizations-and-definitions (accessed on 28 November 2024).
19. Gounella, R.H.; Leite, I.S.; Inada, N.M.; Carmo, J.P.P.D. Wireless Portable Evaluation Platform for Photodynamic Therapy: In Vitro Assays on Human Gastric Adenocarcinoma Cells. *IEEE Sens. J.* **2020**, *20*, 13950–13958. [CrossRef]
20. Marciniak, T. Application of the Nucleo STM32 module in teaching microprocessor techniques in automatic control. *Prz. Elektrotech.* **2022**, *1*, 247–250. [CrossRef]
21. Indriyani, Y.A.; Efendi, R.; Rustami, E.; Rusmana, I.; Anwar, S.; Djajakirana, G. Affordable ESP32-based monitoring system for microbial fuel cells: Real-time analysis and performance evaluation (ESP32-based data logger as a monitoring system for microbial fuel cell). *Int. J. Energy Water Resour.* **2023**, *8*, 199–212. [CrossRef]
22. De Campos da Costa, J.P.; Bastos, W.B.; da Costa, P.I.; Zaghete, M.A.; Longo, E.; Carmo, J.P. Portable Laboratory Platform with Electrochemical Biosensors for Immunodiagnostic of Hepatitis C Virus. *IEEE Sens. J.* **2019**, *19*, 10701–10709. [CrossRef]
23. Da Costa, J.P.D.C.; Gounella, R.H.; Bastos, W.B.; Longo, E.; Carmo, J.P. Photovoltaic Sub-Module With Optical Sensor for Angular Measurements of Incident Light. *IEEE Sens. J.* **2019**, *19*, 3111–3120. [CrossRef]
24. Gomes, J.M.; Correia, J.H.; Carmo, J.P. A Low-Cost Flexible-Platform (LCFP) for characterization of photodetectors. *Measurement* **2015**, *61*, 206–215. [CrossRef]

25. Powell, A. Democratizing production through open source knowledge: From open software to open hardware. *Media Cult. Soc.* **2012**, *34*, 691–708. [CrossRef]

26. Pearce, J. *OPEN-SOURCE LAB: How to Build Your Own Hardware and Reduce Research Costs*; ScienceDirect: Amsterdam, The Netherlands, 2013. Available online: https://www.sciencedirect.com/book/9780124104624/open-source-lab (accessed on 28 November 2024).

27. Espressif. ESP32-WROOM-32 Datasheet. Available online: https://www.espressif.com/sites/default/files/documentation/esp32-wroom-32_datasheet_en.pdf (accessed on 28 November 2024).

28. Espressif. ESP-NOW Wireless Communication Protocol | Espressif Systems. Available online: https://www.espressif.com/en/solutions/low-power-solutions/esp-now (accessed on 28 November 2024).

29. Hernández-Rodríguez, E.; Amalia, R.; Schalm, O.; Alain Martínez Hernández, L.; Daniellys Alejo Sánchez Janssens, T.; Jacobs, W. Reliability Testing of a Low-Cost, Multi-Purpose Arduino-Based Data Logger Deployed in Several Applications Such as Outdoor Air Quality, Human Activity, Motion, and Exhaust Gas Monitoring. *Sensors* **2023**, *23*, 7412. [CrossRef]

30. Yadav, A.; Sakle, N. Development of a low-cost data logger system for capturing transmission parameters of two-wheelers using Arduino. *Mater. Today Proc.* **2022**, *72*, 1697–1703. [CrossRef]

31. Analog.com. MAX4466. 2021. Available online: https://www.analog.com/en/products/max4466.html#part-details (accessed on 21 October 2024).

32. Analog.com. MAX6675 Datasheet and Product Info | Analog Devices. 2021. Available online: https://www.analog.com/en/products/max6675.html (accessed on 28 November 2024).

33. Digital Metal-Oxide Multi-Gas Sensor ENS160 ENS160 Datasheet. Available online: https://www.sciosense.com/wp-content/uploads/2023/12/ENS160-Datasheet.pdf (accessed on 21 October 2024).

34. Analog.com. DS3231 Datasheet and Product Info | Analog Devices. 2024. Available online: https://www.analog.com/en/products/ds3231 (accessed on 28 November 2024).

35. Amorim, M.L.M.; Lima, J.D.; Torres, N.N.S.; Hartmann, L.V.; Salvadori, F.; Ando Junior, O.H. Open-Source Code: Data Logger System for Monitoring and Fault Detection in Bench Testing. *Zenodo* **2024**. [CrossRef]

36. Han, D.; Jiaqiang, E.; Deng, Y.; Chen, J.; Leng, E.; Liao, G.; Zhao, X.; Feng, C.; Zhang, F. A review of studies using hydrocarbon adsorption material for reducing hydrocarbon emissions from cold start of gasoline engine. *Renew. Sustain. Energy Rev.* **2021**, *135*, 110079. [CrossRef]

37. Krishnasamy, A.; Gupta, S.K.; Reitz, R.D. Prospective fuels for diesel low temperature combustion engine applications: A critical review. *Int. J. Engine Res.* **2020**, *22*, 2071–2106. [CrossRef]

38. Balasingam, B.; Ahmed, M.; Pattipati, K. Battery Management Systems—Challenges and Some Solutions. *Energies* **2020**, *13*, 2825. [CrossRef]

39. TensorFlow. TensorFlow. 2019. Available online: https://www.tensorflow.org/ (accessed on 28 November 2024).